NUMERICAL SIMULATION OF THERMAL EFFICIENCY OF AN INNOVATIVE Al_2O_3 NANOFLUID SOLAR THERMAL COLLECTOR
Influence of Nanoparticles Concentration

by

Gianpiero COLANGELO*, Marco MILANESE, and Arturo DE RISI

Department of Engineering for Innovation, University of Salento, Lecce, Italy

Original scientific paper
https://doi.org/10.2298/TSCI151207168C

Investigations on the potential thermal efficiency of an innovative nanofluid solar thermal collector have been performed using a commercial software (RadTherm ThermoAnalytics rel. 10.5). The Al_2O_3-nanofluid has been simulated as working fluid of the solar thermal collector, varying the nanoparticles concentration from 0%vol of Al_2O_3 nanoparticles (pure water) up to 3%vol of Al_2O_3 of nanoparticles. The numerical model has been validated with experimental data, obtained with a real prototype of the simulated solar thermal collector. Real thermal properties of the nanofluids at different concentrations have been used in the simulations. The boundary conditions used for the simulations have been those of real weather conditions. An increase in thermal efficiency (up to 7.54%) has been calculated using nanofluid with a volume fraction of 3% and the influence of nanoparticles concentration on the thermal performance of the solar collector has been pointed out.

Key words: *thermal modeling, heat transfer, solar collector, nanofluids, efficiency*

Introduction

Nanofluids are one of the most promising technologies for increasing the performance of heat transfer fluids [1-3]. Colangelo *et al.* [1, 4] investigated the performance enhancement of nanofluids, used as heat transfer fluids, based on water and diathermic oil. A cooling system that used Al_2O_3-water nanofluid, able to increase the efficiency of a wind turbine was investigated by de Risi *et al.* [5]. The effects of using nanofluids inside solar systems were investigated by Lu *et al.* [6]. They used water-CuO nanofluids in an evacuated tubular solar air collector, integrated with simplified compound parabolic concentrator (CPC) and a special open thermosyphon. The mean evaporating heat transfer coefficient on the spirally coiled tube was calculated for water-CuO nanofluids, with a mass fraction between 0.8%wt and 1.5%wt. Results were compared with heat transfer coefficient obtained with pure water. In their work the heat transfer coefficient was directly proportional to the mass fraction of solid phase for values up to 1.2%wt. Chougule *et al.* [7] studied efficiency of heat pipe solar collector, with pure water and water-CNT nanofluid. For this purpose, two identical set-ups were built and the working fluid was water in one set-up and water-CNT 0.15%vol nanofluid in the

* Corresponding author, e-mail: gianpiero.colangelo@unisalento.it

other one. The effects of a solar tracker and tilt angle were investigated. With 50° tilt angle for both water and nanofluid as working fluid the best results have been obtained. Besides solar tracker increases efficiency of heat-pipe solar collectors. Efficiency of heat-pipe solar collector *vs*. reduced temperature differences has been analyzed. Results showed that water-CNT nanofluid increased efficiency up to 10%, compared to that obtained by using pure water. The use of nanofluids in solar thermal systems, as heat transfer fluid, is a very promising solution to improve the overall efficiency, as proved by many recent works [8-16]. On the other hand, nanofluids revealed some technical issues in traditional solar flat panel, because of nanoparticles sedimentation, as highlighted in the work of Colangelo *et al*. [17]. One of the modern approach to implement the thermal model of a solar thermal collector is the discretized thermal model and it is at the basis of a numerical solution. Klein *et al*. [18] developed a lumped model considering the heat transfer fluid temperature variation along the collector. This model, *1n-node model*, is discretized as an unsteady energy balance for each point. Kamminga [19] considered, instead, the thermal capacitance of the fluid in a *3n-node model*: absorber, cover and heat transfer fluid. Considering also the capacitance of the thermal insulation of the collector, it is a *4n-node model*. The thermal profile of the discretized model results from a set of linear PDE, simplified into ordinary PDE, solved by means of numerical Runge-Kutta method [20]. Oliva *et al*. [21] developed a numerical method based on a 4n-node model: the thermal inertia of the components is considered and the heat transfer fluid is calculated solving the Navier-Stokes equations, with a finite volume approach. Taylor *et al*. [22] demonstrated that nanofluids, used as working fluid in a receiver of a concentrating solar thermal system, can increase efficiency up to 10.0%, if compared to traditional fluids. Otanicar *et al*. [23] investigated the effects of water based nanofluids with silver nanoparticles in a direct absorption solar collector, obtaining an improved efficiency, dependent on particle size. Yousefi *et al*. [24] considered nanofluids improvements in a flat solar collector, using water-Al_2O_3 nanofluid with a weight fraction of 0.2%. They obtained enhancement of efficiency of 28.3%, in comparison with water, and by using a surfactant the efficiency enhanced was 15.63%. The technical issue of sedimentation phenomenon, which can be detected in solar collectors was faced by Colangelo *et al*. [17]. To avoid this problem, they proposed a modified flat plate solar collector, in order to maintain a constant flow velocity along both bottom and top header. In this paper the investigation is, therefore, focused on thermal modeling of a flat solar thermal collector, with the same geometrical characteristics of the solar collector built by Colangelo *et al*. [17]. The goal is to evaluate the efficiency, by using bi-distilled water and Al_2O_3 nanofluid with different nanoparticles concentrations as heat transfer fluid and to evaluate the influence of the concentration on the thermal performance of the system with the same boundary conditions. For this purpose, four different nanofluid concentrations have been simulated as working fluid in the system: 0%vol, 1%vol, 2%vol, and 3%vol.

Solar collector and model description

The thermal model of the solar thermal collector has been implemented with RadTherm (ver. 10.5, Thermoanalytics Inc., USA) [25], that is a thermal analyzing software based on finite element method analysis. Thermal models in RadTherm are based on surface mesh and organized into a hierarchical arrangement of nodes, elements, parts, and assemblies. The energy balance is based on combination of radiation, convection, and conduction. Environmental effects are also included as boundary conditions. Each element in the surface mesh shows two sides (front and back) separated by a specified thickness and has an associated thermal node. The energy equation is then discretized by using the Crank-Nicholson implicit

finite difference scheme, which is second-order accurate in time and space [26]. RadTherm allows considering a variable solar irradiance and variable weather conditions (ambient temperature, wind speed, and direction). Therefore, simulations have been performed taking into account real environmental conditions. The solar collector is made of a Cu absorber, two header tubes and nine riser tubes. For both top and bottom header, Cu tubes with inner diameter of 20 mm and thickness of 1 mm, respectively, have been considered, while Cu tubes with inner diameter of 10 mm and thickness of 1 mm, respectively, have been modeled for riser tubes. The tubes are welded on a 1332 × 860 mm Cu plate and coated with black paint. A shaped element is inserted inside the top and bottom header to maintain a constant flow velocity in order to avoid sedimentation phenomenon. The absorber is inserted inside a galvanized steel frame, covered with a polycarbonate plate and insulated with 22 cm thick glass wool and polyurethane panel. The heat transfer fluid inside the solar collector is a nanofluid consisting of a dispersion of variable concentration of Al_2O_3 nanoparticles having a nominal diameter of 45 nm in bi-distilled water.

The following assumptions have been made.

– Uniform and constant temperature at the inlet of the solar thermal collector.
– The nanofluid is considered as a homogeneous mixture.
– No dust is deposited on the collector surface.
– The junctions between Cu plate and Cu riser tubes are perfectly adhering.
– The solar collector is facing south without external shading.
– Hourly data for solar radiation, air temperature and wind speed were collected by a weather station, installed in city of Lecce (south of Italy) on the structure of the experimental set-up.
– The simulations have been carried out under steady-state conditions, according to standard EN 12975–2. Thermal solar systems and components – Solar collectors – Part 2: Test methods [27].

The solar collector has been modeled with a mesh made of 194405 shell elements, as reported in fig. 1, where it is possible to see the model in the RadTherm environment with the protective transparent polycarbonate cover (a) and without this component (b).

The mathematical model performs the energy balance of the solar collector. The energy balance considers the total irradiance incident on the collector, the optical losses, the thermal losses and the thermal energy transferred to the nanofluid. Heat transfer by conduction to the panel structural frame is often ignored because of the small area of contact. However, in this work, it is considered throughout the RadTherm software. Steady-state heat conduction is computed with eq. (1):

$$\nabla(k\nabla T) = 0 \qquad (1)$$

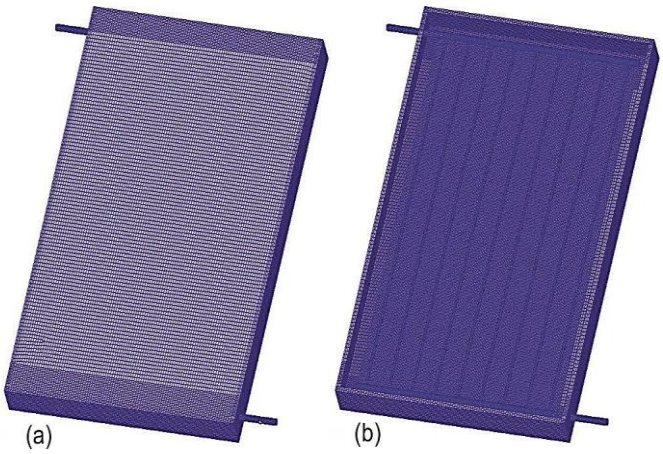

Figure 1. Mesh of the model; (a) with protective polycarbonate cover, (b) without cover

A schematic picture of the computational layers of a section of the model of the thermal collector, as shown in fig. 1, and of the main energy fluxes are shown in fig. 2. A part of the incident solar energy is absorbed by the polycarbonate layer, $q_{\text{sol_plc}}$. The radiation transmitted through the polycarbonate, $q_{\text{sky_rad}}$, is intercepted by the absorber and then transferred to the heat transfer fluid by convection. The remaining part of energy is retransmitted back via the top of the panel by convection and radiation, U_f, as well as by the back of the panel, U_b, and heat loss through thermal bridges at the junctions, $U_{\text{loss_bridge}}$.

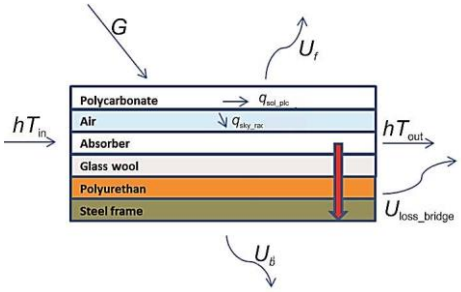

Figure 2. Layers and main energy fluxes of the solar collector model

Heat transfer through the polyurethane, wool glass mattress and the structure of panel occurs both for convection and conduction. The mechanism of the convective heat transfer depends on the pressure inside the section between the two surfaces. At low pressures the heat transfer is mainly due to molecular conduction but at high pressures natural convection is prevalent. Radiation is always present and represents the most important contribution in heat transfer. Between the external surface and the atmosphere, heat is exchanged for both convection and radiation. Radiative heat transfer, due to the temperature difference between the outer surface and the sky, is evaluated approximating the panel as a small gray and convex surface in a large cavity, approximated as a black body (the sky). RadTherm considers multimode heat transfer, taking into account the not homogeneous temperature field that is created by the heat transfer fluid, which flows from the inlet to the outlet of the absorber piping. RadTherm numerically solves the continuity and momentum equations, which governs the fluid flow, as in eqs. (2) and (3):

$$\nabla(\rho u) = 0 \tag{2}$$

$$\frac{\partial u}{\partial t} + u\nabla u = -\frac{1}{\rho}\nabla p + \frac{\mu}{\rho}\nabla^2 u \tag{3}$$

The heat transfer equation is also solved for heat transfer in the flowing fluid into the Cu piping, as shown in eq. (4):

$$\rho c_p u \nabla T = \nabla(k \nabla T) \tag{4}$$

The density of the nanofluids has been calculated using the formula given by eq. (5) [28]:

$$\rho_{\text{nf}} = (1-\varphi)\rho_{\text{fl}} + \varphi\rho_{\text{p}} \tag{5}$$

The specific heat of the nanofluid has also been calculated using the formula [28] in eq. (6):

$$c_{\text{nf}} = (1-\varphi)c_{\text{fl}} + \varphi c_p \tag{6}$$

The correlation, that was used here, is:

$$c_{\text{nf}} = \frac{(1-\varphi)\rho_{\text{fl}}c_{\text{fl}} + \varphi\rho_{\text{p}}c_p}{\rho_{\text{nf}}} \tag{7}$$

Viscosity increase, as a function of volume concentration, is obtained by the Einstein eq. (8) [29, 30], for dilute non-interacting suspensions of spherical particles:

$$\mu_{\mathrm{i}} = \mu_{\mathrm{r}} - 1 = 2.5\varphi \tag{8}$$

Where μ_{r} is the so-called relative viscosity given by eq. (9):

$$\mu_{\mathrm{i}} = \frac{\mu}{\mu_0} \tag{9}$$

where φ is the particle volume concentration. It can be seen that nanofluid viscosity increases with increasing of nanoparticle concentration in a non-linear manner and the Einstein equation greatly under predicts the nanofluid values, although the equation has shown to be able to predict the viscosity of suspensions with a volume concentration up to 10% with an uncertainty less than 6%, as demonstrated by Goodwin and Hughes [31].

Regression of the experimental data of Chen *et al*. [32] gives the eq. (10):

$$\mu_{\mathrm{i}} = \mu_{\mathrm{r}} - 1 = 10.6\varphi + (10.6\varphi)^2 \tag{10}$$

The bi-nomial relationship between the viscosity variation and the nanoparticle volume concentration is similar to that for aqueous-based Al_2O_3 nanofluids [33, 34] and EG-based Al_2O_3 nanofluids [34]. For thermal conductivity properties of nanofluid made of commercial Al_2O_3 nanoparticles and bi-distillated water, the experimental measures, contained in Colangelo *et al*. [1], have been considered. Nanoparticles have a spherical shape, a density of 3700 kg/m^3 and an average diameter of 45 nm. In particular, considering bi-distilled water as base fluid, volume fraction of Al_2O_3 particles of 3% gives an enhancement of thermal conductivity up to 6.70%. The simulations have been carried out in steady-state conditions, according to EN 12975–2 standard [27] and, therefore, efficiency of solar thermal collector has been calculated.

The power extracted by solar collector, is calculated with eq. (11):

$$q = \dot{m} c_p \left(T_{\mathrm{out}} - T_{\mathrm{in}}\right) \tag{11}$$

where q can also be obtained through efficiency, η:

$$q = G\eta \tag{12}$$

Efficiency is represented as a function of T_m^*, reduced temperature difference:

$$T_m^* = \left[\frac{(T_{\mathrm{in}} + T_{\mathrm{out}})}{2} - t_{\mathrm{a}}\right]\frac{1}{G} \tag{13}$$

RadTherm allows calculating the temperature profile of a component or part of it. The result of each simulation is, therefore, the temperature profile of the solar thermal collector, in particular the temperature T_{out}.

Simulated cases

The simulated cases in RadTherm were summer and winter solstices, in which heat transfer fluid has been changed in order to determine thermal efficiency, tab. 1. The test is performed by measuring T_m^*, in clear sky condition, for four levels of temperature of inlet fluid. The inlet temperature has been set at 30 °C, 45 °C, 55 °C, and 65 °C, respectively, at

summer and winter solstice. Flow rate of 0.02 kg/s has been considered, as that used to investigate sedimentation of nanofluid inside solar collector with transparent tubes [17], and real weather data were considered as air temperature, wind speed, solar radiation, *etc*. The solar collector has been simulated with a tilt angle of 30° at summer solstice and of 50° at winter solstice. A summary of the properties of materials is shown in tab. 2.

Table 1. Summary of test cases

Case	Period	Tin fluid	Tilt
1	Summer solstice	30°C	30°
2	Summer solstice	45°C	30°
3	Summer solstice	55°C	30°
4	Summer solstice	65°C	30°
5	Winter solstice	30°C	50°
6	Winter solstice	45°C	50°
7	Winter solstice	55°C	50°
8	Winter solstice	65°C	50°

Model validation

The validation of the thermal model has been obtained with experimental data, acquired during the prototype testing. The experimental set-up to measure the efficiency of the flat panel solar thermal collector is based on the EN 12975-2 standard [27]: efficiency measurements shall be made over a temperature range between ambient temperature and 80 °C, under clear sky conditions [35]. In the experimental tests, inlet temperature of solar collector is adjusted by band heaters, controlled by a PID circuit, whereas thermal equilibrium is guaranteed by a shell and tube heat exchanger and an air-water heat exchanger. The Pt100 sensors are used to measure both inlet and outlet temperature of solar collector and heat exchanger. The system measures direct irradiance and diffuse irradiance on solar collector by means of pyranometers. The efficiency, calculated with the temperature, measured with thermocouples at the outlet of solar collector prototype in a clear-sky day of summer solstice (total solar radiation of 920 W/m^2, flow-rate of 0.02 kg/s), is reported in fig. 3. With the same test conditions, thermal simulations have been performed and their results are presented in fig. 3 as well. The errors between experimental data and calculated results with RadTherm are reported in tab. 3. The model yields results with an acceptable error if compared with experimental data.

Table 2. Material properties – solar thermal collector

	Material	ρ, [kgm^{-3}]	k, [Wm^{-1}K^{-1}]	c_p, [Jkg^{-1}K^{-1}]
Transparent sheet	Polycarbonate	1200	0.2	1300
Absorber	Cu	8954.35	Function of temperature	Function of temperature
Insulation sheet 1	Glass wool	960	0.3	2300
Insulation sheet 2	Polyurethane	1200	0.35	2090
Galvanized box	Steel	7817	Function of temperature	Function of temperature

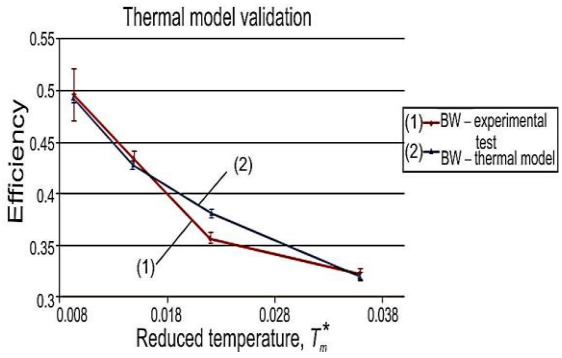

Figure 3. Thermal model validation

Table 3. Error – thermal model validation

	T_{in} [°C]	T_{out} [°C]	ΔT_{out} [°C]	T_m^*	η	η – error
1 – Model	30.5	36.56	0.04	0.0093	0.492	0.37%
1 – Experimental	30.5	36.60		0.0093	0.496	
2 – Model	45	50.26	0.07	0.0148	0.428	0.61%
2 – Experimental	45	50.34		0.0149	0.434	
3 – Model	52	56.69	0.30	0.0221	0.381	2.47%
3 – Experimental	52	56.39		0.0220	0.357	
4 – Model	65	68.94	0.03	0.0359	0.320	0.21%
4 – Experimental	65	68.96		0.359	0.322	

Results and discussion

As described previously, simulations have been carried out in significant days: summer and winter solstices. Efficiency of solar thermal collector has been calculated in a post processing session, according to EN 12975–2 standard [27], in clear sky conditions for four levels of temperature of the inlet fluid. Efficiency of solar thermal collector at its corresponding T_m^* is reported in tab. 4 for summer solstice and in tab. 5 for winter solstice. In summer simulations the ambient air temperature is 30 °C and the global solar irradiance is 920 W/m^2. From the data reported in tab. 4, when the inlet temperature of bi-distilled water (BW) is 30 °C, the outlet temperature is 36.56 °C, corresponding to a thermal efficiency of 0.492. The thermal efficiency increases when the Al_2O_3 nanofluid is used, yielding the benefit in terms of thermal efficiency increase of 3.054% for a volume concentration of 1% of Al_2O_3 nanoparticles, 5.528% for a volume concentration of 2% and up to 7.384% for a volume concentration of 3%. In the second level of temperature, when the inlet temperature is T_{in} = 45 °C, the outlet temperature of bi-distilled water is 50.26 °C, corresponding to a thermal efficiency of about 0.428. When the heat transfer fluid is the nanofluid, 1% of Al_2O_3, the gain in efficiency is comparable to previous case and it is of 2.66%. The increase in thermal efficiency grows up with the nanofluid concentration and it is 4.802% with a volume fraction of 2% and it becomes 6.829% when using a nanofluid with a volume fraction of 3% on Al_2O_3 nanoparticles. The third level of inlet temperature (55 °C), in summer solstice, is the typical working temperature of solar thermal collector for residential use. In this case the output temperature of bi-distilled water is 56.69 °C, obtaining a thermal efficiency of the solar collector of 0.389. Even if these data could appear a low value if compared to commercial solar collectors, they are acceptable because the panel is homemade and therefore is less efficient. The main aim of this investigation is not about the absolute performance of thermal solar collector, but about the influence of the usage of nanofluids in such a system and how the overall efficiency is increased. In this case, using nanofluid with a volume fraction of 1% increases efficiency of 2.045%. Using nanofluids with higher volume fractions leads to better performance. With 2%vol Al_2O_3 nanofluid the increase in efficiency is 3.805%, while 3%vol Al_2O_3 nanofluid the increase in efficiency is 6.431%. When the working fluid enters at 65 °C the working conditions of the thermal panel are hard and the outlet temperature of bi-distilled water is about 69 °C, with an efficiency of 0.320. The benefit in terms of thermal efficiency increase is 1.563%, when 1%vol Al_2O_3 nanofluid is used, while it is 3.884% and 5.038% for the other investigated concentrations. Winter simulations results are shown in tab. 5. When the inlet temperature

Table 4. Results – summer solstice

Fluid	T_{in} [°C]	T_{out} [°C]	T_m^*	η	$\Delta\eta$
BW	30	36.56	0.0093	0.492	–
1%-Al_2O_3	30	36.99	0.0095	0.523	3.054%
2%-Al_2O_3	30	37.36	0.0097	0.548	5.528%
3%-Al_2O_3	30	37.65	0.0099	0.566	7.384%
BW	45	50.26	0.0148	0.428	–
1%-Al_2O_3	45	50.64	0.0150	0.455	2.660%
2%-Al_2O_3	45	50.96	0.0152	0.476	4.802%
3%-Al_2O_3	45	51.15	0.0156	0.496	6.829%
BW	55	56.69	0.0226	0.389	–
1%-Al_2O_3	55	56.84	0.0233	0.410	2.045%
2%-Al_2O_3	55	57.12	0.0234	0.427	3.805%
3%-Al_2O_3	55	57.51	0.0235	0.454	6.431%
BW	65	68.94	0.0359	0.320	–
1%-Al_2O_3	65	69.17	0.0360	0.336	1.563%
2%-Al_2O_3	65	69.49	0.0362	0.359	3.884%
3%-Al_2O_3	65	69.68	0.0363	0.371	5.038%

Table 5. Results – winter solstice

Fluid	T_{in} [°C]	T_{out} [°C]	T_m^*	η	$\Delta\eta$
BW	30	35.30	0.0219	0.394	–
1%-Al_2O_3	30	35.63	0.0220	0.417	2.302%
2%-Al_2O_3	30	35.87	0.0222	0.433	3.886%
3%-Al_2O_3	30	36.22	0.0224	0.458	6.386%
BW	45	48.86	0.0372	0.316	–
1%-Al_2O_3	45	49.09	0.0372	0.331	1.474%
2%-Al_2O_3	45	49.47	0.0370	0.355	3.886%
3%-Al_2O_3	45	49.67	0.0371	0.368	5.162%
BW	55	55.44	0.0447	0.282	–
1%-Al_2O_3	55	55.60	0.0448	0.293	1.045%
2%-Al_2O_3	55	55.88	0.0450	0.313	3.046%
3%-Al_2O_3	55	56.10	0.0451	0.328	4.577%
BW	65	68.02	0.0588	0.248	–
1%-Al_2O_3	65	68.19	0.0589	0.259	1.115%
2%-Al_2O_3	65	68.29	0.0596	0.268	1.997%
3%-Al_2O_3	65	68.58	0.0591	0.287	3.861%

of the heat transfer fluid is 30 °C, the outlet temperature, in the case of bi-distilled water, is 35.30 °C that corresponds to a thermal efficiency of 0.394. Thermal efficiency of the panel is lower than in the summer solstice simulations: this is mainly due to the ambient temperature of about 13 °C and consequently to the higher thermal losses. In the simulations performed in winter solstice, the thermal efficiency increases with the volume concentration of nanopowder as well.

The increase is about 2.302% for volume concentration of 1% of Al_2O_3, 3.886% for volume concentration of 2% of Al_2O_3 nanoparticles and 6.386% for volume concentration of 3%. In the second winter test case the inlet temperature of the heat transfer fluid is 45 °C. When the fluid is bi-distilled water, thermal efficiency is 0.316 and the benefit in terms of increase in efficiency, when 1%vol. nanofluid flows, is 1.475%. As in other simulated cases, the efficiency gain increases with the nanofluid volume concentration: for 2%vol. nanofluid it is 3.886% and for 3%vol. nanofluid it is 5.162%. In the simulations with inlet temperature of 55 °C and 65 °C the difference of temperature with the external environment gives lower efficiencies and the efficiency benefit, due to the use of nanofluid, is lower as well. The solar thermal collector efficiency in terms of T_m^* for all the simulated cases is represented in fig. 4, where it is possible to see the behavior of the collector by using different nanofluid volume fractions. It is evident that using Al_2O_3 nanofluids improves the thermal efficiency of the solar collector and in particular the efficiency increases with the nanoparticles volume fraction.

Conclusion

A new type of thermal solar collector working with water-Al_2O_3 nanofluid has been modeled with RadTherm ThermoAnalytics release 10.5. In particular, after the validation of the model a set of simulations has been performed in order to investigate the influence of the nanofluid volumetric concentration on the thermal performance of the solar collector. All the

simulations have been performed with real weather conditions in the city of Lecce, Italy considering four levels of temperature of inlet fluid in summer and winter solstices. The simulations were carried out to model the heat transfer in the solar thermal collector and to determine the gained thermal efficiency of using nanofluids instead of traditional working fluid. Nanofluids have shown an improvement of solar thermal collector behavior that is dependent on the nanoparticle concentration and on the reduced temperature. In particular, the increase of thermal efficiency is better for high nanoparticle concentration and for low values of the reduced temperature, leading to a maximum increase of 7.54% compared to bi-distilled water as working fluid. This study will be a guide for the design of the experimental campaign that will be performed on the real prototype in order to record data in different seasons and environmental conditions.

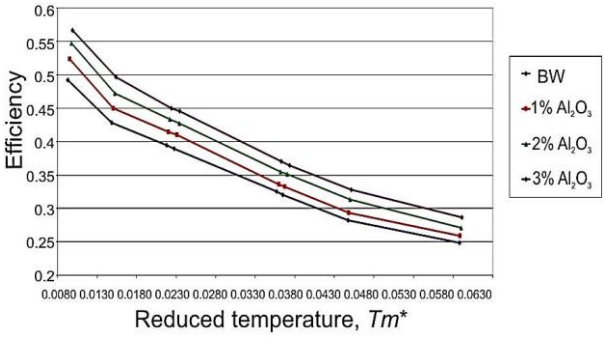

Figure 4. Thermal efficiency *vs* . reduced temperature, T_m^*

Nomenclature

A – surface area, [m^2]
c_p – specific heat, [Jkg^{-1}K^{-1}]
D – inside diameter, [m]
G – solar radiation, [Wm^{-2}]
h – heat transfer coefficient, [Wm^{-2}K^{-1}]
k – thermal conductivity, [Wm^{-1}K^{-1}]
L – characteristic length, [m]
$\dot{m}$ – flow-rate, [kgs^{-1}]
q_i – heat *i* mode, [Wm^{-2}]
p – pressure
s – thickness of the *i* material, [m]
T_i – temperature at *i* node, [K]
t_a – ambient temperature, [ºC]
u – flow velocity, [ms^{-1}]
U_i – heat transfer coefficient, [Wm^{-2}K^{-1}]

Greek symbols

η – efficiency
μ – viscosity of suspension, [Pa s]
ρ – fluid density, [kgm^{-3}]
φ – nanoparticle volumetric fraction

Subscripts

a – available
b – back of panel
bridge – thermal bridge and junction
f – front of panel
fl – heat transfer fluid
i – increase
in – inlet
loss – thermal loss
nf – nanofluid
out – outlet
p – nanoparticle
plc – polycarbonate sheet
r – relative
rad – radiative heat transfer mode
sky – sky
sol – solar

References

[1] Colangelo, G., *et al*., Results of Experimental Investigations on the Heat Conductivity of Nanofluids Based on Diathermic Oil for High Temperature Applications, *Applied Energy, 97* (2012), Sept., pp. 828-833
[2] Lomascolo, M., *et al*., Review of Heat Transfer in Nanofluids: Conductive, Convective and Radiative Experimental Results, *Renewable and Sustainable Energy Reviews, 43* (2015), Mar., pp. 1182-1198
[3] Mahian, O., *et al*., A Review of the Applications of Nanofluids in Solar Energy, *International Journal of Heat and Mass Transfer, 57* (2013), 2, pp. 582-594
[4] Colangelo, G., *et al*., Thermal Conductivity, Viscosity and Stability of Al_2O_3-Diathermic Oil Nanofluids for Solar Energy Systems, *Energy, 95* (2016), Jan., pp. 124-136

[5] De Risi, A., *et al*., High Efficiency Nanofluid Cooling System for Wind Turbines, *Thermal Science, 18* (2014), 2, pp. 543-554
[6] Liu, Z.-H, *et al*, Thermal Performance of an Open Thermosyphon Using Nanofluid for Evacuated Tubular High Temperature Air Solar Collector, *Energy Conversion and Management, 73* (2013), Sept., pp. 135-143
[7] Chougule, S.-S, *et al*., Performance of Nanofluid-Charged Solar Water Heater by Solar Tracking System, *Proceedings*, International Conference on Advances in Engineering, Science and Management (ICAESM -2012), Nagapattinam, Tamil Nadu, India, 2012.
[8] Salavati Meibodi, S., *et al*., Experimental Investigation on the Thermal Efficiency and Performance Characteristics of a Flat Plate Solar Collector Using SiO_2/EG-Water Nanofluids, *International Communications in Heat and Mass Transfer, 65* (2015), July, pp. 71-75
[9] Mahian, O., *et al*., Heat Transfer, Pressure Drop, and Entropy Generation in a Solar Collector Using SiO_2/Water Nanofluids: Effects of Nanoparticle Size and Ph, *J. of Heat Transfer, 137* (2015), 6, 061011
[10] Bianco, V., *et al*., Performance Analysis of Turbulent Convection Heat Transfer of Al_2O_3 Water-Nanofluid in Circular Tubes at Constant Wall Temperature, *Energy, 77* (2014), Dec., pp. 403-413
[11] Al-Nimr, M. A., Al-Dafaie, A. M. A., Using Nanofluids in Enhancing the Performance of a Novel Two-Layer Solar Pond, *Energy, 68* (2014), Apr., pp. 318-326
[12] Sardarabadi, M., *et al*., Experimental Investigation of the Effects of Silica/Water Nanofluid on PV/T (Photovoltaic Thermal Units), *Energy, 66* (2014), Mar., pp. 264-272
[13] Mahian, O., *et al*., First and Second Laws Analysis of a Minichannel-Based Solar Collector Using Boehmite Alumina Nanofluids: Effects of Nanoparticle Shape and Tube Materials, *International Journal of Heat and Mass Transfer, 78* (2014), Nov., pp. 1166-1176
[14] Mahian, O., *et al*., Performance Analysis of a Minichannel-Based Solar Collector Using Different Nanofluids, *Energy Conversion And Management, 88* (2014), Dec., pp. 129-138
[15] Mahian, O., *et al*., Entropy Generation During Al_2O_3/Water Nanofluid Flow in a Solar Collector: Effects of Tube Roughness, Nanoparticle Size, and Different Thermophysical Models, *International Journal of Heat and Mass Transfer, 78* (2014), Nov., pp. 64-75
[16] Colangelo, G., *et al*., Innovation in Flat Solar Thermal Collectors: A Review of the Last Ten Years Experimental Results, *Renewable and Sustainable Energy Reviews, 57* (2016), May, pp. 1141-1159
[17] Colangelo, G., *et al*., A New Solution for Reduced Sedimentation Flat Panel Solar Thermal Collector Using Nanofluids, *Applied Energy, 111* (2013), Nov., pp. 80-93
[18] Klein, S., *et al*., Transient Considerations of Flat-Plate Solar Collectors, *Journal of Eng. for Power, 96* (1974), 2, pp. 109-113
[19] Kamminga, W., The Approximate Temperatures within a Flat-Plate Solar Collector under Transient Conditions, *Int. Journal Heat Mass Transf., 28* (1985), 2, pp. 433-440
[20] Butcher, J., *The Numerical Analysis of Ordinary Differential Equations*, John Wiley and Sons, New York, USA, 1987
[21] Oliva, A., *et al*., Numerical Simulation of Solar Collectors: The Effect of Non-Uniformity and Non--Steady State of Boundary Conditions, *Solar Energy, 47* (1991), 5, pp. 359-373
[22] Taylor, R. A., *et al*., Applicability of Nanofluids in Concentrated Solar Energy Harvesting, *Proceedings*, 4th International Conference on Energy Sustainability, Santorini, Greece, 2010, Vol. 1, pp. 825-832
[23] Otanicar, T. P., *et al*., Nanofluid-Based Direct Absorption Solar Collector, *Journal of Renewable and Sustainable Energy, 2* (2010), 3, pp. 2-13
[24] Yousefi, T., *et al*., An Experimental Investigation on the Effect of Al_2O_3-H_2O Nanofluid on the Efficiency of Flat-Plate Solar Collector, *Renewable Energy, 39* (2012), 1, pp. 293-298
[25] ***, www.thermoanalytics.com
[26] Fadugba, S. E., *et al*., Crank Nicholson Method for Solving Parabolic Partial Differential Equations, *IJA2M, 1* (2013), 3, pp. 8-23
[27] ***, Standard EN 12975-2: Thermal Solar Systems and Components – Solar Collectors – Part 2.
[28] Buongiorno, J., Convective Transport in Nanofluids, *Journal of Heat Transfer, 128* (2006), 3, pp. 240-250
[29] Einstein, A., *Eine neue Bestimmung der Molekul-Dimension* (A New Determination of the Molecular Dimensions – in German), *Annalen der Physik, 324* (1906), 2, pp. 289-306
[30] Einstein, A., *Berichtigung zu meiner Arbeit: Eine neue Bestimmung der Molekul-Dimension* (Correction of my Work: A New Determination of the Molecular Dimensions – in German), *Annalen der Physik*, 339 (1911), 3, pp. 591-592

[31] Goodwin, J. W., Hughes, R. W., *Rheology for Chemists—An Introduction*, Royal Society of Chemistry, London, 2000
[32] Chen, H., *et al*., Rheological Behaviour of Nanofluids, *New Journal of Physics, 9* (2007), Oct., pp. 367-391
[33] Das, S. K., *et al*., Temperature Dependence of Thermal Conductivity Enhancement for Nanofluids, *ASME Journal of Heat Transfer, 125* (2003), 4, pp. 567-74
[34] Wang, X. W., *et al*., Thermal Conductivity of Nanoparticle-Fluid Mixture, *Journal of Thermophys. Heat Transfer, 13* (1999), 4, pp. 474-80
[35] Fisher, S., *et al*., Collector Test Method under Quasi-Dynamic Conditions According to the European Standard EN 12975-2, *Solar Energy, 76* (2004), 1-3, pp. 117-123

Paper submitted: December 7, 2015
Paper revised: April 4, 2016
Paper accepted: July 7, 2016

© 2017 Society of Thermal Engineers of Serbia.
Published by the Vinča Institute of Nuclear Sciences, Belgrade, Serbia.
This is an open access article distributed under the CC BY-NC-ND 4.0 terms and conditions.